Limaye, A.B., et al., 2021, River sinuosity describes a continuum between randomness and ordered growth: Geology, v. 49, https://doi.org/10.1130/G49153.1

Supplementary information for "River sinuosity describes a continuum between randomness and ordered growth"

Ajay B. Limaye[1], Eli D. Lazarus[2], Yuan Li[1], and Jon Schwenk[3]

[1]*Department of Environmental Sciences, University of Virginia, Charlottesville, Virginia 22904*

[2]*Environmental Dynamics Lab, School of Geography and Environmental Science, University of Southampton, Highfield, Southampton SO17 1BJ, UK*

[3]*Earth Science Division, Los Alamos National Laboratory, Los Alamos, New Mexico 87545*

METHODS

Mapping natural river centerlines

We analyzed the centerlines for natural channels from an existing global dataset that includes rivers with widths ≥30 m (Allen and Pavelsky, 2018a, 2018b) and targeted datasets for rivers with documented channel migration in the Andean foreland and the continental US (Lagasse et al., 2004; Sylvester et al., 2019). For the Allen and Pavelsky (2018b) dataset, we used their "simplified" centerlines and excluded features flagged as canals, tidal channels, or lakes.

We used spline interpolation to resample the channel centerline data with the node spacing equal to the mean channel width, consistently with the modeled centerlines. A sensitivity test for the global sinuosity dataset showed a difference of < 4% in the median sinuosity using linear (S = 1.40) versus spline interpolation (S = 1.45). We used a fitting procedure to estimate AR-2 model parameters for the interpolated version of each of the natural centerlines (Fig. S1).

Sinuosity calculations

Geologic constraints such as valley margins can steer channels at scales substantially larger than individual meander bends (Ferguson, 1975), which can introduce sources of sinuosity beyond those created by either random perturbations or channel migration. Therefore, to diminish this effect we calculated sinuosity for all modeled and natural channels using the average value for a moving window with width $L = 50w_c$, where L is along-stream distance and w_c is channel width. For a channel with high sinuosity (e.g., $S = 3$), this window scale is slightly greater than the meander wavelength (Williams, 1986).

AR-2 model

Using the second-order autoregressive (AR-2) model, we rendered each channel centerline with a length of 150 channel widths; for natural meanders with sinuosity $S = 1.5$, this length corresponds to roughly 10 meander wavelengths (Williams, 1986). The model is stationary and oscillatory within a region of parameter space bounded by $-1 < b_2 < 1 - |b_1|$ and $b_2 < -\frac{1}{4}b_1^2$ (Ferguson, 1979). We ran a parameter sweep across $0 < b_1 \leq 2.0$ and $-1 \leq b_2 < 0$, which includes this constrained region, and varied σ from 0.1 to 0.5. These ranges span the large majority of fitted AR-2 parameter values for natural channels using the global dataset (Fig. S1).

Each model parameter independently affects centerline shape (Fig. S2). Increasing the magnitude of b_1 increases meander wavelength and sinuosity. Increasing the magnitude of b_2 (i.e., more negative values) decreases meander wavelength, or similarly increases the frequency of curvature change. Increasing σ with other parameters fixed increases sinuosity.

The detailed form of each modeled centerline depends on the random disturbance series ϵ (Equation 1 in the main text). Therefore, for each set of parameters (b_1, b_2 and σ) we used n

different series of ϵ to generate a set of replicate centerlines. We measured the proportion of the channel length that belonged to meander neck cutoffs (i.e., self-intersecting loops), and removed these cutoffs to generate simplified centerlines. Straightened reaches formed by enacting the cutoff were generated with the original node spacing using linear interpolation. Then for each set of replicates, we calculated the mean and standard deviation of sinuosity, the proportion of sinuosity values greater than a critical value (S_c = 1.5), and the mean fraction of original channel length in cutoff loops.

We separately tested the effect of the number of replicate centerlines (n) on estimated sinuosity statistics for the AR-2 model (Fig. S3). Overall, the mean sinuosity for each replicate set is consistent between n = 100 and n = 1000, except for cases in which a significant portion of the modeled centerlines is bound in cutoff loops (Fig. S3A). The standard deviation of sinuosity behaves similarly between the n = 100 and n = 1000 cases (Fig. S3B). We used linear regression to determine the R^2 value for the mean sinuosity calculated for 1000 replicates versus the mean calculated with smaller values of n, excluding any replicate sets that included cutoffs. Figure S3C shows that R^2 does not change substantially for $n \geq 100$ (Fig. S3C). Therefore, we used n = 100 replicates for each parameter set using the AR-2 model for the analyses in the main text (Fig. 2 and 4).

Channel migration model

We modeled river channel migration using the curvature-driven centerline model of Howard and Knutson (1984). In this model, channel width (w_c) is fixed and the centerline evolves due a spatial convolution of local and upstream centerline curvature. The dimensionless migration rate is

$$R_1(s) = \Omega R_o(s) + \frac{\Gamma \int_0^{\xi max} R_o(s-\xi) G(\xi) d\xi}{\int_0^{\xi max} G(\xi) d\xi}, \text{(S1)}$$

where s is the centerline node index, $R_o = (Cw_c)^{-1}$, C is local curvature, ξ is distance along the centerline, and Ω and Γ are weighting coefficients set to -1 and 2.5, respectively. G is a weighting function

$$G(\xi) = e^{-\frac{2kC_f}{h_c}\xi}, \text{(S2)}$$

where k is a dimensionless coefficient set to unity, C_f is a dimensionless friction coefficient set to 0.01 and h_c is channel depth. We set channel width and depth to 20 m and 1 m, respectively. The dimensioned migration rate at each node is calculated as

$$M(s) = k_e R_1(s) \mu^{\varepsilon}, \text{(S3)}$$

where k_e is a rate constant, μ is overall channel sinuosity, and ε is a coefficient set to -2/3. We set k_e to yield a maximum lateral erosion rate of 1 m/year. Meander neck cutoffs were identified by self-intersection of the channel banks and were removed. The model boundary conditions were periodic with respect to channel geometry and the curvature integration (Equation S1). For further details regarding model implementation see Limaye and Lamb (2013).

To characterize the channel centerlines evolved using this model, we measured the length of half-meanders between curvature inflections after Howard and Hemberger (1991). We measured the 84th percentile of half-meander bend length to isolate the behavior of relatively long bends that contribute substantially to overall sinuosity (Fig. 3B in the main text). We also measured sinuosity using the same moving-window approach as for the centerlines from the AR-2 model and natural cases.

REFERENCES CITED

Allen, G.H., and Pavelsky, T.M., 2018a, Global extent of rivers and streams: Science, v. 361, p. 585–588, https://doi.org/10.1126/science.aat0636.

Allen, G.H., and Pavelsky, T.M., 2018b, Global River Widths from Landsat (GRWL) Database (Version V01.01) [Data set]: Zenodo, https://doi.org/10.5281/zenodo.1297434.

Ferguson, R.I., 1975, Meander irregularity and wavelength estimation: Journal of Hydrology, v. 26, p. 315–333, https://doi.org/10.1016/0022-1694(75)90012-8.

Ferguson, R.I., 1979, River meanders: regular or random?, *in* Wrigley, N. ed., Statistical applications in the spatial sciences, London, Pion Limited, p. 229–241.

Howard, A.D., and Hemberger, A.T., 1991, Multivariate characterization of meandering: Geomorphology, v. 4, p. 161–186, https://doi.org/10.1016/0169-555X(91)90002-R.

Howard, A.D., and Knutson, T.R., 1984, Sufficient conditions for river meandering—a simulation approach: Water Resources Research, v. 20, p. 1659–1667, https://doi.org/10.1029/WR020i011p01659.

Lagasse, P.F., Zevenbergen, L.W., Spitz, W.J., and Thorne, C.R., 2004, Methodology for predicting channel migration: Transportation Research Board of the National Academies, https://doi.org/10.17226/23352.

Limaye, A.B.S., and Lamb, M.P., 2013, A vector-based method for bank-material tracking in coupled models of meandering and landscape evolution: Journal of Geophysical Research: Earth Surface, v. 118, p. 2421–2437, https://doi.org/10.1002/2013JF002854.

Sylvester, Z., Durkin, P., and Covault, J.A., 2019, High curvatures drive river meandering: Geology, v. 47, p. 263–266, https://doi.org/10.1130/G45608.1.

Williams, G.P., 1986, River meanders and channel size: Journal of Hydrology, v. 88, p. 147–164, https://doi.org/10.1016/0022-1694(86)90202-7.

FIGURES

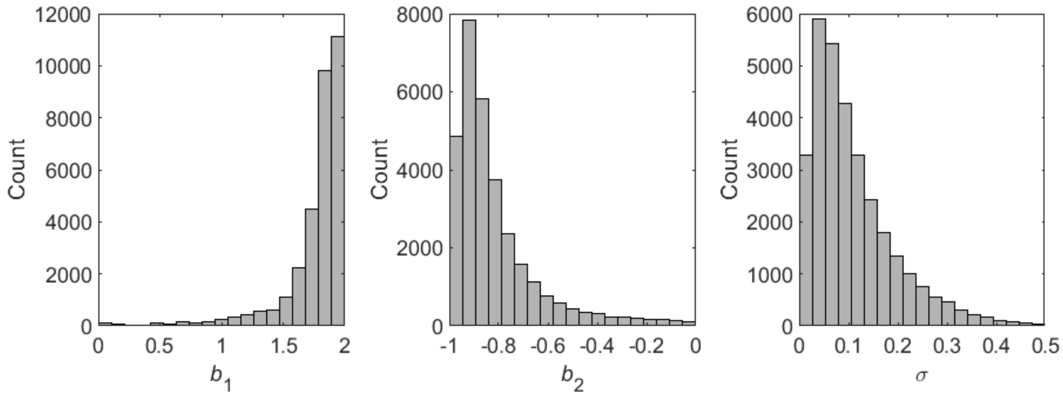

Figure S1. Histograms of fitted AR-2 model parameters (b_1, b_2, σ) for a global dataset of natural channels (Allen and Pavelsky, 2018a, 2018b).

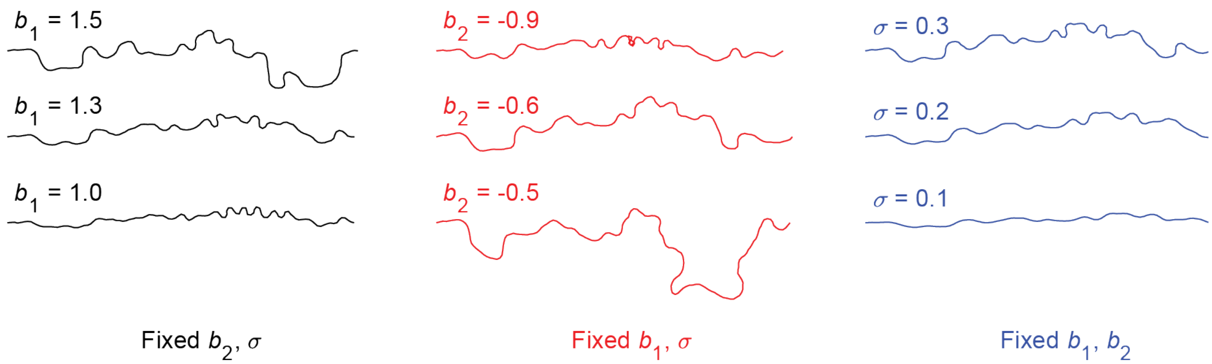

Figure S2. Example channel centerlines for different magnitudes of each of the parameters, b_1, b_2 and σ, with the other two parameters fixed.

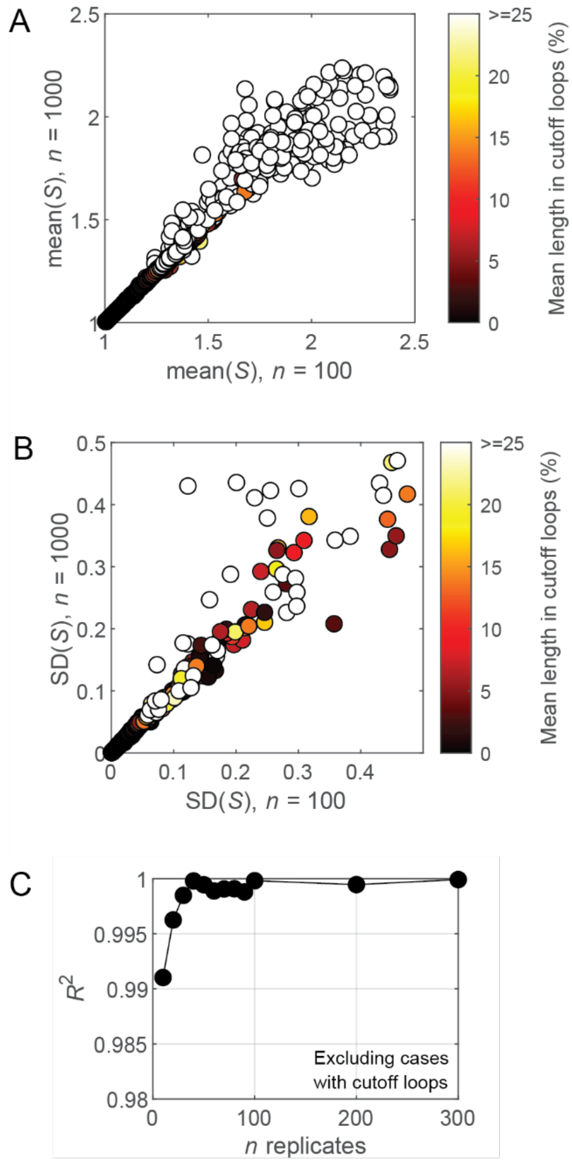

Figure S3. Sensitivity analyses to test the effect of the number replicate centerlines (n) generated using the AR-2 model on estimated sinuosity (S) statistics. (A) Scatter plot of mean sinuosity for each set of replicate centerlines using n =1000 versus n = 100. The marker color indicates the mean length of the original channel in cutoff loops for the n = 1000 cases. (B) Scatter plot of the standard deviation (SD) of sinuosity for n = 1000 versus n = 100. The marker color uses the same convention as in (A). (C) R^2 value for mean(S) using 1000 replicates versus mean(S) using n replicates, plotted against n. This plot excludes any cases with cutoff loops.